Available online at www.sciencedirect.com
SCIENCE DIRECT®
Journal of Photochemistry and Photobiology A: Chemistry 181 (2006) 414–420
Journal of Photochemistry and Photobiology A:Chemistry
www.elsevier.com/locate/jphotochem

Photophysical properties of hydroxyanthraquinone derivatives (HQAs)-doped SiO_2, SiO_2–Al_2O_3 and Al_2O_3 matrices

Dae Won Cho [a,*], Minjoong Yoon [b,**]

[a] *Department of Chemistry, Seonam University, Namwon, Jeonbuk 590-711, Republic of Korea*
[b] *Department of Chemistry, Chungnam National University, Daejeon 305-764, Republic of Korea*

Received 10 September 2005; received in revised form 14 December 2005; accepted 24 December 2005

Abstract

Transparent inorganic matrix materials such as SiO_2, SiO_2–Al_2O_3 and Al_2O_3, which were chemically doped with hydroxyanthraquinone derivatives (HAQs) such as 1-HAQ and 1,4-dihydroxyanthraquinone (1,4-DHAQ) were prepared using a sol–gel technique. In SiO_2 system, the absorption spectra of 1-HAQ and 1,4-DHAQ were observed to show the absorption maxima around 420 nm by red-shift and blue-shift from those observed in toluene, respectively, whereas those of both HAQs were red-shifted in both SiO_2–Al_2O_3 and Al_2O_3 matrices. These results indicate that chemical interactions of HAQs in SiO_2 system are different from those in Al_2O_3 and SiO_2–Al_2O_3 matrices, which play important role in electronic structural changes in the intramolecular hydrogen bonding of HAQs. All the HAQs-doped matrix systems showed the markedly Stokes-shifted emission spectra which are originated from the excited-state intramolecular proton transfer (ESIPT) in HAQs. Based on the emission lifetimes of HAQs in each matrix, the ESIPT of HAQs was found to be inhibited by the chemical interaction with Al in the Al_2O_3-related matrices such as SiO_2–Al_2O_3 and Al_2O_3.

Keywords: Hydroxyanthraquinones; Alumina; Silica; Organic–inorganic hybrid matrix; Excited-state intramolecular proton transfer

1. Introduction

Organic–inorganic hybrid materials have been attracting a great deal of attention because novel material properties can be produced through systematic design of the organic and inorganic complexes [1]. The sol–gel processes have been widely used to prepare the organic–inorganic hybrid materials [2,3], where metal alkoxide solutions containing functional organic molecules are used as the starting materials. Concurrently, the research on the polymerization of metal alkoxide has led to development of optically interesting materials such as solid laser dye blocks and films [4], photochromic glasses, hole-burning materials [5], light guides, and nonlinear optical materials [6].

Most studies of the organic–inorganic hybrid compounds have been performed concerning different properties depending on doping methods. For example, the hybrid materials prepared mostly by physical doping of the organic compound have demonstrated that the dopants are present as individual molecules in the inorganic matrix, retaining their properties in the matrix as in the solution [7,8]. In other words, the functionalities of dopants are retained even in the solid state, allowing the physically doped materials to be used in various applicable devices. Alternatively, the organic–inorganic hybrid materials have been known to be efficiently prepared by doping through formation of chemical bonds between organic guests and inorganic hosts. This preparation method has been regarded as one of the promising directions for the new design and improvements of properties in the hybrid materials [9–11]. In this regard, hydroxyanthraquinone derivatives (HAQs) have attracted a great attention as a useful dopant in the Si–Al binary oxide systems, which would improve optical properties [9]. Actually, HAQs have been served as model systems for the chromophore of biological and pharmaceutical interest including the antitumor antibiotics and the lysozime inhibitors [12]. Also, the HAQs have been applied as dispersed dyes for coloring synthetic polymer materials [13]. The steady-state emission spectra

---

* Corresponding author at: Department of Chemistry, Chosun University, Gwangju 501-759, Republic of Korea.
** Co-corresponding author.
E-mail addresses: dwcho@seonam.ac.kr (D.W. Cho), mjyoon@cnu.ac.kr (M. Yoon).

1010-6030/$ – see front matter © 2005 Elsevier B.V. All rights reserved.
doi:10.1016/j.jphotochem.2005.12.027

of HAQs show a characteristic dual emission. This phenomenon has been interpreted in terms of the excited state intramolecular proton transfer (ESIPT) [14,15]. 1-Hydroxyanthraquinone (1-HAQ) in solution has a weak normal fluorescence together with a markedly Stokes-shifted emission which is attributed to a tautomer species formed upon ESIPT. The ESIPT of the chromophore is usually affected by a certain chemical environmental change. However, no systematic studies have been done on the photophysical properties of HAQs in inorganic matrices related to the ESIPT process as well as chemical bonding with matrices in spite of the possibility of covalent binding of HAQs with the inorganic systems.

In the present study, we synthesized the transparent HAQs-doped SiO_2, SiO_2–Al_2O_3 and Al_2O_3 matrices by the sol–gel process, and their photophysical properties related to the chemical interaction of HAQs with the inorganic matrices were investigated in terms of the ESIPT process by using the absorption and fluorescence spectral techniques.

2. Experimental

In this work, 1-hydroxyanthraquinone (1-HAQ) and 1,4-dihydroxyanthraquinone (1,4-DHAQ) were used as organic dopants, which were purchased from Aldrich Chemical Co. and further purified by several times of recrystallization. Tetraethoxysilane (TEOS) and $Al(OBu\text{-}s)_3$ were purchased from the Aldrich Co. and used without further purification.

The HAQs/SiO_2–Al_2O_3 matrix system was synthesized through preparation of homogeneous solution by two-step hydrolysis of tetraethoxysilane (TEOS) and $Al(OBu\text{-}s)_3$, since the rate of hydrolysis of both alkoxides are different. As a prehydorlysis solution, a mixture of TEOS, H_2O and HCl in ethanol was used. After holding the prehydrolysis solution at 40 °C for 24 h, $Al(OBu\text{-}s)_3$ dissolved in ethanol stock solution of HAQs, and HCl was added to the prehydorlysis solution. The final mixed solution was kept at 30 °C for about a week to form a transparent gel product. The chemical compositions of the products are listed in Table 1. HAQs-doped SiO_2 and Al_2O_3 systems were also prepared by hydrolysis of TEOS and $Al(OBu\text{-}s)_3$, separately, and by mixing with ethanol solution of HAQs similarly to the above procedure. The surface morphologies of the synthesized matrixes coated on quartz glass were characterized by measuring the scanning electron microscopic (SEM) image using the field-emission scanning electron microscope (Hitachi, S-4700).

In order to characterize optical properties of the matrixes, diffuse reflectance absorption spectra of were recorded by using a Shimadzu UV-3101PC spectrophotometer equipped with an integrating sphere, in which absorbance were evaluated by the Kubelka–Munk functional analysis. The measurements of fluorescence spectra were performed with a CCD detector (Princeton Instruments, Inc.; SpectraMax RTEA/CCD-128-H), a monochromator (Acton Research Corporation; SpectraPro-300i) and a He:Cd laser (Omnichrome; Series 74) to excite the samples.

Temporal profiles of the fluorescence decays were measured by using time-correlated single photon counting method (TCSPC). The excitation source is a self-mode-locked picosecond Ti:sapphire laser (Coherent Co.) pumped by an $Nd:YVO_4$ laser. Laser output has a ~3 ps pulse width, and it can span the excitation wavelength in the range 350–490 nm by second-harmonic generation. All the standard electronics for the TCSPC were from the Edinburgh Instruments. The instrumental response function was measured by detecting the scattered laser pulse of ca. 3 ps with quartz crystal. The resultant FWHM is 60 ps. This method allows a time resolution of about 30 ps after deconvolution.

Table 1
Compositions of the starting materials of the Al/Si binary oxides (molar ratio)

	TEOS	Ethanol	H_2O	HCl	$Al(OBu\text{-}s)_3$	HAQs
A	1	8	2	10^{-4}	$\sim10^{-2}$	10^{-5}
B	1	8	2	10^{-4}	$\sim10^{-3}$	10^{-5}
C	1	8	2	10^{-4}	$\sim10^{-2}$	10^{-4}

3. Results and discussion

3.1. Synthesis and characterization of HAQs-doped matrices

Fig. 1 shows the SEM images of the HAQs-doped inorganic matrices. Generally, the particle sizes of SiO_2 matrix are much smaller than those of Al_2O_3 matrix. It is noteworthy that the particle sizes of the binary oxide SiO_2–Al_2O_3 system were observed to be in between those of SiO_2 and Al_2O_3. This implies that two-step hydrolysis plays an important role in the synthetic routes, considering the fact that the hydrolysis rate of $Al(OBu\text{-}s)_3$ is faster than TEOS. Actually the particle size can be controlled by reducing the reagent concentrations and reaction time. However, in this study, we keep the same synthetic conditions such as the concentration and reaction time for all the matrices in order to study the composition dependency of the spectroscopic properties (vide infra). Therefore, throughout the experiment, the particle size of the Al_2O_3 is kept larger than that of SiO_2 or SiO_2–Al_2O_3 system as shown in SEM images, even if Al_2O_3 system is optically semitransparent as compared to the transparent SiO_2 or SiO_2–Al_2O_3 system

3.2. Absorption spectral properties

The diffuse reflectance absorption spectra of 1-HAQ and 1,4-DHAQ doped in various inorganic matrices are shown in Fig. 2. The spectroscopic properties are summarized in Table 2. The absorption spectrum of 1-HAQ in SiO_2 matrix look similar to that observed in toluene [16–18], showing the absorption max-

Table 2
Absorption and fluorescence maxima (nm) of each system

	In toluene		SiO_2		Al_2O_3		SiO_2–Al_2O_3	
	Abs	Flu	Abs	Flu	Abs	Flu	Abs	Flu
1-HAQ	408	585	415	571	478	581	415	571
1,4-DHAQ	483	570	420	571	554	625	518	604

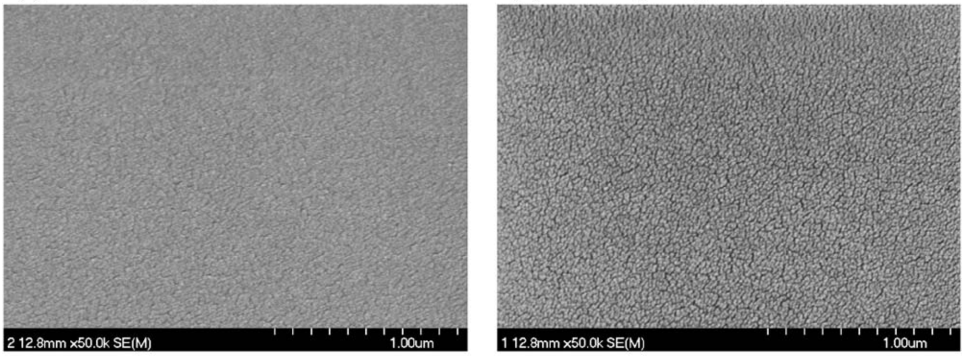
(a). 1-HAQ/SiO_2 (b). 1-HAQ/SiO_2-Al_2O_3

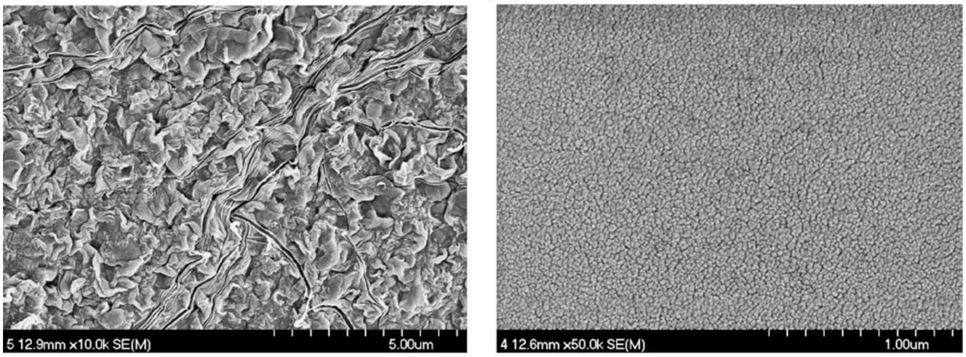
(c). 1-HAQ/Al_2O_3 (d). 1,4-DHAQ/SiO_2

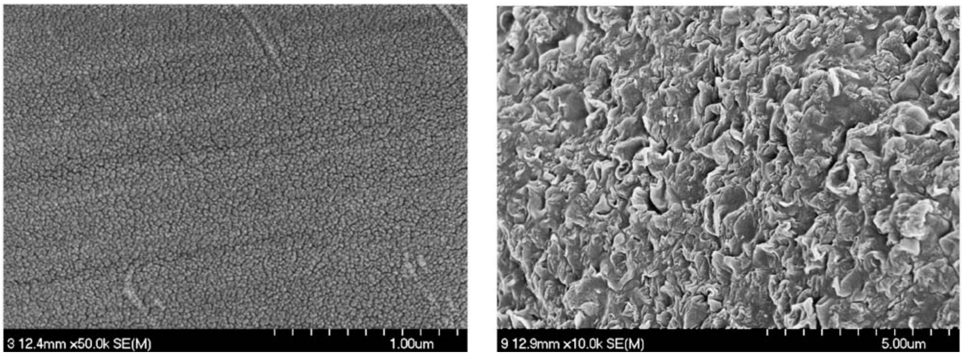
(e). 1,4-DHAQ/SiO_2-Al_2O_3 (f). 1,4-DHAQ/Al_2O_3

Fig. 1. SEM images of various HAQs in inorganic matrices: (a) 1-HAQ/SiO_2, (b) 1-HAQ/SiO_2–Al_2O_3, (c) 1-HAQ/Al_2O_3, (d) 1,4-DHAQ/SiO_2, (e) 1,4-DHAQ/SiO_2–Al_2O_3, and (f) 1,4-DHAQ/Al_2O_3.

imum around 415 nm which is slightly red-shifted from that observed in toluene (408 nm) (Table 2). This is probably due to weak interaction of 1-hydroxyl group of 1-HAQ with SiO_2. As shown in Fig. 3, 1-HAQ in nonpolar toluene can form a closed configuration through intramolecular hydrogen bonding. However, in SiO_2 matrix, the closed configuration would be partially changed to an open configuration by the competitive interaction of carbonyl group of 1-HAQ with OH of SiO_2 surface.

On the other hand, the absorption maximum of 1,4-DHAQ in toluene was observed at much longer wavelength as compared to that of 1-HAQ in toluene. This must be due to the highly delocalized electronic structures of the closed configuration formed through the double intramolecular hydrogen bonding in nonpolar solvent. This closed configuration can be also changed into the open configuration in SiO_2 matrix as in the case of 1-HAQ. This is why the absorption maximum of 1,4-DHAQ in SiO_2 matrix is rather blue-shifted to 420 nm which is similar to that observed for the open configuration of 1-HAQ in SiO_2 matrix. In contrast to the different absorption spectral changes in SiO_2 matrix, the absorption maxima of both HAQs in Al_2O_3 matrix were markedly red-shifted by 70 nm from those of toluene solution, indicating that the interaction patterns of the two HAQs with Al_2O_3 matrix are different from the competitive hydrogen bonding interactions of HAQs with SiO_2 matrix. Bräuchle et al. [19,20] have proposed the chemical binding model for the 1,4-DHAQ/γ-A12O3 system, i.e., one proton of 1,4-DHAQ forming an intramolecular hydrogen bond was replaced by an Al atom. Thus, it can be inferred that the interaction of HAQs with Al_2O_3 matrix must be a chemical bonding, ligation of Al with carbonyl group and hydroxyl group as shown in Fig. 3.

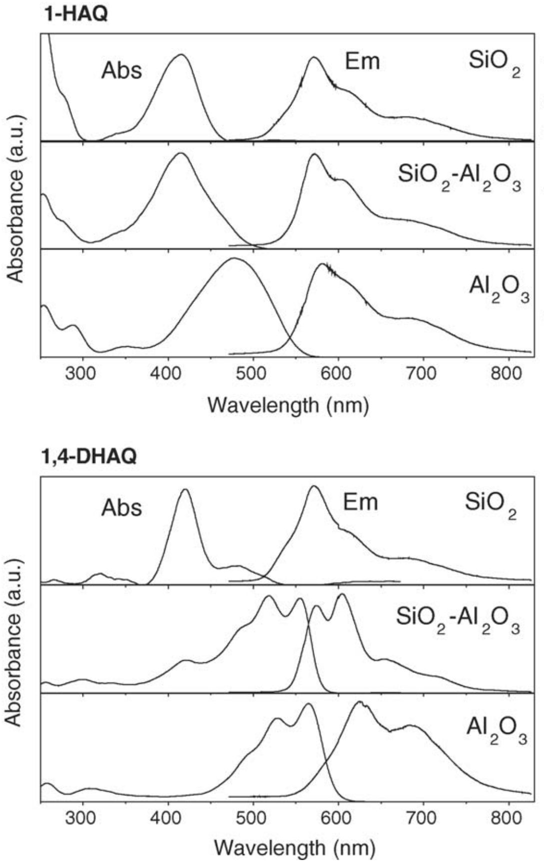

Fig. 2. Absorption and fluorescence spectra of 1-HAQ (upper) and 1,4-DHAQ (bottom) in SiO_2, SiO_2–Al_2O_3 and Al_2O_3 matrices, respectively. Solid lines: SiO_2, dotted lines: SiO_2/Al_2O_3, and dash-dotted lines: Al_2O_3.

Actually, the HAQs were not observed to be extracted from the HAQs-doped Al_2O_3 kept in nonpolar solution such as $CHCl_3$, supporting that HAQs are chemically bound with Al in Al_2O_3 matrix. The chemical ligation keeps the closed configuration of HAQs so that the delocalized electron distribution is more available to be energetically stabilized to exhibit the red-shift of the absorption band. Further, the absorption band-shifts of substituted anthraquinone are known to be dependent on the electron donation power of the substituent, and it is believed that the electron donating character of Al is also responsible for the red-shifts in the absorption spectra.

The absorption spectrum of 1-HAQ in SiO_2–Al_2O_3 system was observed to be the same as that observed in SiO_2 matrix, indicating that the intermolecular hydrogen bonding of 1-HAQ with SiO_2 is still dominant in the binary matrix. However, the absorption spectrum of 1,4-DHAQ in SiO_2–Al_2O_3 system exhibited red-shifted band at long wavelength (518 nm) which is shorter than that observed in pure Al_2O_3 system. This implies that a partial ligation of 1,4-DHAQ with Al (Fig. 3(B)) is available in competition with intermolecular hydrogen bonding with a portion of SiO_2. This may be because 1,4-DHAQ has two symmetric ligation sites, C_9=O···OH and C_{10}=O···OH in contrast to 1-HAQ containing one ligand which is rather sensitive to the intermolecular hydrogen bonding to form the open configuration. In other words, 1-HAQ interacts with SiO_2 more easily than with Al_2O_3, but 1,4-DHAQ has one more ligand to form Al-complex by overcoming the competition with intermolecular hydrogen bonding with SiO_2. This is consistent with the previous report that the absorption band around 480 nm is decreased and a new absorption is appeared around 560 nm with an increase in concentration of Al_2O_3 [9]. The red-shift of the absorption band was also reported to be completed when the [Al]/[1,4-DHAQ] ratio exceeded about 700 [9]. Thus, it can be inferred that

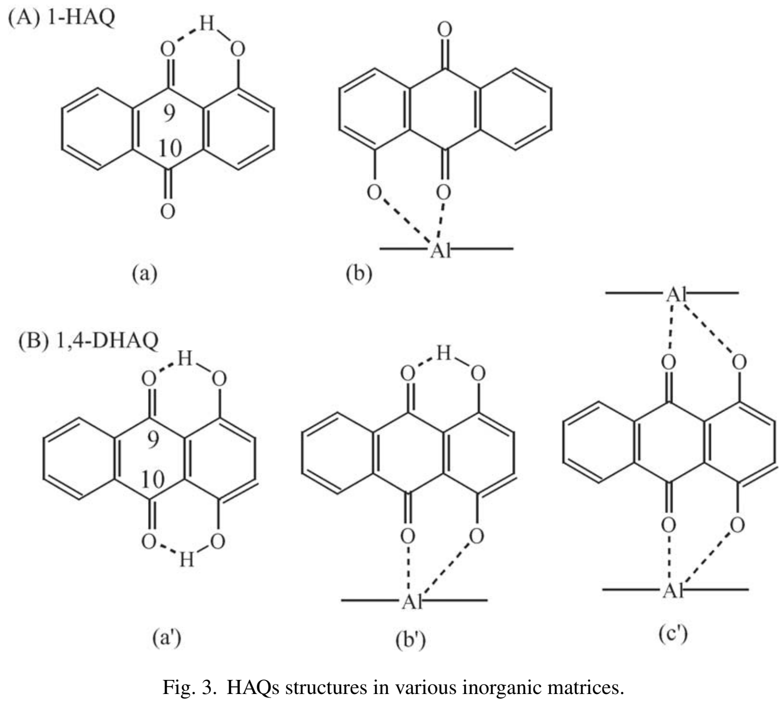

Fig. 3. HAQs structures in various inorganic matrices.

the spectrum of 1,4-DHAQ in SiO_2–Al_2O_3 system was formed by the mixture of each spectrum for 1,4-DHAQ/SiO_2 and 1,4-DHAQs/Al_2O_3 systems.

3.3. Fluorescence spectral properties

The fluorescence spectra of both 1-HAQ and 1,4-DHAQ doped in a SiO_2 matrix were observed to show broad and intense emission bands beyond 571 nm with a weak shoulder at ca. 530 nm, exhibiting a large Stokes shift (ca. 6500 cm^{-1}) as shown in Fig. 2. These spectral features are similar to that in toluene solution [16–18], and the large Stokes-shifted bands are attributed to the emission from an excited *keto*-tautomer formed via excited-state intramolecular proton transfer (ESIPT) process [16–18]. This indicates that the intramolecular hydrogen bonding is mostly retained to form a closed configuration of HAQs in SiO_2 matrix in spite of a little open configuration formed through intermolecular hydrogen bonding interaction with SiO_2 as discussed above. Consequently, the weak 530 nm emission is originated from the excited *enol*-tautomers. Although the absorption spectra of HAQs are markedly red-shifted in Al_2O_3 systems, the Stokes shift of the emission spectra is much reduced as compared to that observed in SiO_2, implying that the ESIPT is inhibited by the Al-ligation which interrupts the intramolecular hydrogen bonding as shown in Fig. 3. The Stokes-shift observed for 1,4-DHAQ (ca. 2000 cm^{-1}) is smaller than that observed for 1-HAQ (ca. 3700 cm^{-1}). This reduced Stokes shift was observed even in the binary SiO_2–Al_2O_3 matrix system, although it is ca. 2900 cm^{-1} which is in between the values observed separately in SiO_2 and Al_2O_3. These observations again indicate that Al-ligation plays an important role in interrupting the intramolecular hydrogen bonding facilitating ESIPT.

In order to confirm the steady-state spectroscopic studies, the emission decay profiles of HAQs doped in different inorganic matrices were measured, and they were observed to strongly depend on the matrix nature such as SiO_2, SiO_2–Al_2O_3 and Al_2O_3 as shown in Figs. 4 and 5. The fluorescence decays were analyzed to fit exponential functions following a deconvolution procedure, using a proper instrument response function. The goodness of the fits was judged from the reduced χ^2 values and the distribution of the weighted residuals among the data channels. For all the accepted fits, the χ^2 values were within 1.30, and the weighted residuals were randomly distributed among the data channels used. The analyzed decay times are summarized in Table 3. In case of HAQs/SiO_2 matrix, the emission decay profiles observed at 500, 600 and 700 nm were well fitted into a single exponential function (Figs. 4(a)–(c) and 5(a)). The probe wavelengths were selected to confirm the electronic states from the structural band. One measured at 500 nm is mainly responsible for emission decay profiles of *enol*-tautomer. The decay profile of *enol*-tautomer in the early decay time looks like the instrumental response function of the current TCSPC system. This result indicates that the fluorescence lifetime of *enol*-tautomer is shorter than 30 ps, which is consistent the low fluorescence intensity of *enol*-tautomer. Meanwhile, the emission decay profiles of 1-HAQ/SiO_2 (Fig. 4(b) and (c)) and 1,4-DHAQ/SiO_2 (Fig. 5(a)) measured at both 600 and/or 700 nm exhibit an identical decay time constants of 0.44 and 1.5 ns, respectively, which were mainly attributed to *keto*-tautomer emission. Therefore, the fine structures of *keto*-tautomer emission with ca. 1530 cm^{-1} (Fig. 2) must be originated from the

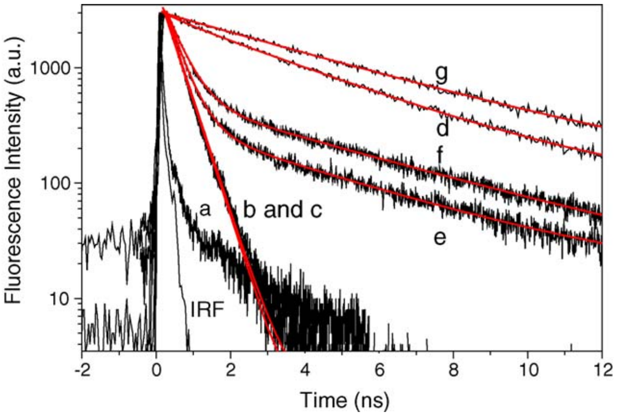

Fig. 4. Fluorescence decay profiles of 1-HAQ in various inorganic matrices: in SiO_2, monitored at 500 nm (a), at 600 nm (b) and 700 nm (c); in SiO_2–Al_2O_3, (sample A) molar ratio 1-HAQ/SiO_2/Al_2O_3 = 10^{-5}/1/10^{-2} (d), (sample B) molar ratio 1-HAQ/SiO_2/Al_2O_3 = 10^{-5}/1/10^{-3} (e), (sample C) molar ratio 1-HAQ/SiO_2/Al_2O_3 = 10^{-4}/1/10^{-2} (f); in Al_2O_3 (g).

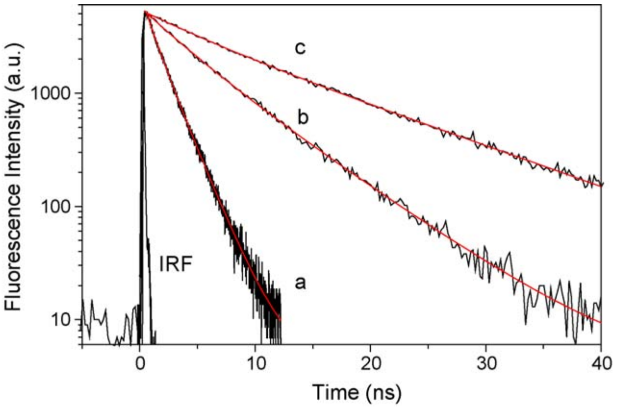

Fig. 5. Fluorescence decay profiles of 1,4-DHAQ in various inorganic matrices monitored at 600 nm: (a) in SiO_2, (b) in Al_2O_3, and (c) in SiO_2–Al_2O_3.

Table 3
Fluorescence lifetimes (ns) of each system monitored at 600 nm

	SiO_2	SiO_2–Al_2O_3			Al_2O_3
		A	B	C	
1-HAQ	0.44 (100)[a]	0.42 (27), 4.9 (73)	0.43 (94), 4.7 (6)	0.46 (89), 4.7 (11)	4.6 (100)
1,4-DHAQ	1.5 (100)	5.3 (36), 12.9 (64)	–	–	12.3 (11), 4.5 (89)

[a] Also monitored at 600 and 700 nm.

aromatic ring-stretching vibrational mode. It is also noteworthy that there is an apparent rise component with time constant shorter than 30 ps (reliable time limit for our apparatus), indicating that an emissive *keto*-tautomer in SiO_2 matrix is formed by ESIPT process as in nonpolar toluene [16–18]. These results suggest that most of HAQs is physically doped in SiO_2 matrix with a little intermolecular hydrogen bonding with SiO_2 as discussed from the absorption spectroscopic results, and the emission of *keto*-tautomer is dominant.

On the other hand, in Al_2O_3 matrix systems, the observed fluorescence decay time-profile of 1-HAQ (Fig. 4(g)) was also analyzed to be single exponential with a decay time of 4.6 ns whereas that of 1,4-DHAQ was biexponential with two decay times of 12.3 and 4.5 ns. These decay times were much longer than the short decay times (0.4 or 1.5 ns) of the *keto*-tautomer observed in SiO_2, indicating that the ESIPT is completely inhibited by formation of Al-complex through ligation of Al with C=O and OH groups as predicted from the absorption spectroscopic studies.

The 4.6 ns decay component for 1-HAQ should be originated from one Al-complex species formed through ligation with C=O···OH as shown in Fig. 3(b), and the 12.3 and 4.5 ns components of 1,4-DHAQ originated from two different Al-complexes formed by ligation with two C=O–H as shown in Fig. 3(b′) and (c′). These Al-complex forms the closed configuration so that the molecular structure is rigid enough to reduce the vibrational energy loss, increasing the fluorescence decay times.

Fig. 4(d)–(f) shows the fluorescence decay profiles of 1-HAQ fitted into the biexponential function of ∼0.42 and ∼4.9 ns with a rise time in the SiO_2–Al_2O_3 matrix (Table 3). The short decay time is similar to that measured in SiO_2 matrix whereas the long decay time is similar to that observed in Al_2O_3, and the short and long decay components should be originated from the *keto*-tautomer formed by ESIPT and the Al-complex, respectively. The relative amplitudes of these two components were observed to depend on the composition of the SiO_2–Al_2O_3 matrix as shown in Table 3, even though the decay times were kept almost constant. For instance, the sample B and C containing high ratio of Al/Si than that of sample A (Table 1) were observed to exhibit higher amplitude of the long decay component, indicating the portion of Al-complex is relatively increased. These results suggest that ESIPT of 1-HAQ is still possible partially in SiO_2–Al_2O_3 matrix in spite of the Al-complex formation to interrupt the ESIPT. However, in case of 1,4-DHAQ doped in SiO_2–Al_2O_3 matrix, the ESIPT seemed to be completely inhibited, since only long decay times of 5.3 and 12.9 ns were observed even in the sample A containing lowest ratio of Al/Si, similarly to those observed from Al_2O_3 matrix. This is consistent with the observation from the steady-state fluorescence spectrum. This implies again that ligation of Al with two C=O···OH groups of 1,4-DHAQ is more competitive with the intermolecular hydrogen bonding with SiO_2 than that of 1-HAQ containing one C=O···OH group. Furthermore, the emission decay times of 1,4-DHAQ were also observed to be identical when monitoring at 570, 620 and 700 nm as the maxima position of fine structures. Thus, these emission bands are assigned to vibrational structure at same excited electronic state, indicating the vibrational structures originated from the anthraquinone ring stretching modes. Thus, it is inferred that the vibrational energy loss is reduced dominantly without ESIPT if the number of Al-ligation site of the chromophore is increased in the binary matrix.

4. Conclusions

In this work, transparent SiO_2, SiO_2–Al_2O_3 and Al_2O_3 matrices doped by HAQs such as 1-HAQ and 1,4-DHAQ were synthesized by the sol–gel method. The different chemical interactions of the doped HAQs depending on the matrices were observed to cause different electronic structural changes in the intramolecular hydrogen bonding of HAQs. Thus, the ESIPT properties of HAQs are strongly affected by the different interactions between HAQs and matrices. The ESIPT of HAQs was found to be inhibited by forming a closed configuration of Al-complex in the Al_2O_3-related matrices such as SiO_2–Al_2O_3 and Al_2O_3, whereas it is not affected in SiO_2. The Stokes-shifted ESIPT emission of HAQs doped in Al_2O_3-related matrices can be controlled by the ratio of Al, because of the inhibition of ESIPT process. All matrices have good optical transparency, so the photophysical properties of HAQs easily can be characterized using the spectroscopic method. This allows us to design new optical materials with HAQs doped in Al_2O_3-related matrices.

Acknowledgements

This work was supported by KOSEF (R05-2001-000-00182-0). Authors also thank Center for Research Facilities of Chungnam National University for operating of the ps-time-resolved fluorescence systems.

References

[1] (a) R.M. Laine, C. Sanchez, C.J. Brinker, E. Giannelis, Organic/Inorganic Hybrid Materials, vol. 519, Materials Research Society, Warrendale, PA, 1998;
(b) L.C. Kelin, L.F. Francis, M.R. De Duire, J.E. Mark, Organic/Inorganic Hybrid Materials II, vol. 576, Materials Research Society, Warrendale, PA, 1999;
(c) R.M. Laine, C. Sanchez, C.J. Brinker, E. Giannelis, Organic/Inorganic Hybrid Materials-2000, vol. 628, Materials Research Society, Warrendale, PA, 2000;
(d) C. Sanchez, R.M. Laine, S. Yang, C.J. Brinker, Organic/Inorganic Hybrid Materials-2002, vol. 726, Materials Research Society, Warrendale, PA, 2002;
(e) C. Sanchez, U. Schubert, R.M. Laine, Y. Chujo, Organic/Inorganic Hybrid Materials-2004, vol. 847, Materials Research Society, Warrendale, PA, 2004;
(f) T. Keeling-Tucker, J.D. Brennan, Chem. Mater. 13 (2001) 3331.
[2] D. Avnir, V.R. Kaufman, R. Reisfeld, J. Non-Cryst. Solids 74 (1985) 395.
[3] J.I. Zink, B.S. Dunn, J. Ceram. Soc. Jpn. 99 (1991) 878.
[4] R. Reisfeld, Proc. SPIE 29 (1990) 1328.
[5] T. Tani, H. Namikawa, K. Arai, J. Appl. Phys. 58 (1985) 3559.
[6] B. O'Regan, M. Gratzel, Nature 353 (1991) 737.
[7] J. Zhang, H. Yamashita, M. Anpo, Chem. Lett. (1997) 1027.
[8] J. Zhang, M. Matsuoka, H. Yamashita, M. Anpo, Langmuir 15 (1999) 77.

[9] T. Ishiwaki, H. Inoue, A. Makishima, J. Non-Cryst. Solids 203 (1996) 43.

[10] F. Chapul, J.-P. Boilol, D. Riehl, Y. Lévy, Sol–Gel Opt. III (1994) 286.

[11] T. Suratwala, Z. Gardlund, J.M. Boulton, D.R. Uhlmann, Sol–Gel Opt. III (1991) 310.

[12] W.A. Remers, The Chemistry of Antitumor Antibiotics, vol. 1, John Wiley, New York, 1979.

[13] R.S. Asquith, P. Ingham, J. Soc. Dyes Colour 94 (1978) 12.

[14] M.H. Van Benthem, G.D. Gillispie, J. Phys. Chem. 88 (1984) 2954.

[15] S.J. Formoshinho, L.G. Arnaut, J. Photochem. Photobiol. A: Chem. 75 (1993) 21.

[16] J.R. Choi, S.C. Jeoung, D.W. Cho, Bull. Korean Chem. Soc. 24 (2003) 1675.

[17] J.R. Choi, S.C. Jeoung, D.W. Cho, Chem. Phys. Lett. 385 (2004) 384.

[18] D.W. Cho, S.H. Kim, M. Yoon, S.C. Jeoung, Chem. Phys. Lett. 391 (2004) 314.

[19] B. Sauter, T. Basché, C. Bräuchle, J. Opt. Soc. Am. B9 (1992) 804.

[20] T. Basché, C. Bräuchle, Chem. Phys. Lett. 181 (1991) 179.